PROCEEDINGS
Of SPIE-The International Society for Optical Engineering

Volume 428

Optical Materials and Process Technology for Energy Efficiency and Solar Applications

Carl M. Lampert
Chairman/Editor

Cooperating Organizations
Department of Energy, Office of Solar Heat Technologies
International Solar Energy Society
American Solar Energy Society

August 23-25, 1983
San Diego, California

Proceedings of SPIE—The International Society for Optical Engineering

Volume 428

Optical Materials and Process Technology for Energy Efficiency and Solar Applications

Cooperating Organizations
Department of Energy, Office of Solar Heat Technologies
International Solar Energy Society
American Solar Energy Society

Carl M. Lampert
Chairman/Editor

August 23-25, 1983
San Diego, California

Published by
SPIE—The International Society for Optical Engineering
P.O. Box 10, Bellingham, Washington 98227-0010 USA
Telephone 206/676-3290 (Pacific Time) • Telex 46-7053

The papers appearing in this book comprise the proceedings of the meeting mentioned on the cover and title page. They reflect the authors' opinions and are published as presented and without change, in the interests of timely dissemination. Their inclusion in this publication does not necessarily constitute endorsement by the editors or by SPIE.

Please use the following format to cite material from this book:
Author(s), "Title of Paper," *Optical Materials and Process Technology for Energy Efficiency and Solar Applications,* Carl M. Lampert, Editor, Proc. SPIE 428, page numbers (1983).

Library of Congress Catalog Card No. 83-051016
ISBN 0-89252-463-4

Printed in the United States of America.

OPTICAL MATERIALS AND PROCESS TECHNOLOGY FOR ENERGY EFFICIENCY AND SOLAR APPLICATIONS

Volume 428

Conference Committee

Chairman
Carl M. Lampert
Lawrence Berkeley Laboratory

Co-Chairmen
David Allred
Energy Conversion Devices, Inc.

Claes G. Granqvist
Chalmers University of Technology, Sweden

Gottfried Haacke
American Cyanamid Co.

Richard B. Pettit
Sandia National Labs.

Stephen E. Selkowitz
Lawrence Berkeley Laboratory

Session Chairmen
Session 1—Heat Mirrors and Optical Switching Films
Gottfried Haacke, American Cyanamid Co.
Carl M. Lampert, Lawrence Berkeley Laboratory

Session 2—Photovoltaic Related Materials and Instrumentation
David Allred, Energy Conversion Devices, Inc.

Session 3—General Solar Optical Coatings and Instrumentation
Richard B. Pettit, Sandia National Labs.

Session 4—Selective Absorber Coatings
Claes G. Granqvist, Chalmers University of Technology, Sweden

OPTICAL MATERIALS AND PROCESS TECHNOLOGY FOR ENERGY EFFICIENCY AND SOLAR APPLICATIONS

Volume 428

INTRODUCTION

A broad range of topics was covered by this conference on solar optical films and coatings for architectural windows and lighting usage. These specialized coatings can significantly improve the energy efficiency and performance of building components and solar energy systems. Many of the topics dealt with new materials or advanced methods to improve known materials. Important and timely research on films, photovoltaic related materials, selective absorbers, fluorescent concentrators, reflectors, and antireflective coatings was described as was essential diagnostic instrumentation.

The session on heat mirrors and optical switching materials included research progress on single-layer highly doped semiconductors along with multiple layer, dielectric/reflector/dielectric, and all dielectric heat mirrors. The design of the reflector layer has been extended beyond metals to include metal nitrides. The concept of utilization of electrochromism for a switchable solar glazing was introduced. This phenomenon has potential for the development of large-scale electronic window shutters. Finally, angle-selective surfaces were demonstrated to have the ability to be sensitive to the incident directon of radiation energy.

Two other sessions were on photovoltaics and general solar coatings. A highlight was the discussion on the mass production of amorphous silicon photovoltaics on flexible metal substrates. Properties of new fluorescent concentrators and photoelectrochemical anodes were covered along with photovoltaic diagnostic methods. Coatings for reflectors, antireflectance, and radiative cooling were discussed in terms of durability and performance. Other issues covered honeycomb insulation and optical measurements.

The final technical session was devoted to solar absorbers. Theoretical viewpoints of possible a/e ratios and graded cermet materials were presented. Variations of black copper, stainless steel and molybdenum were covered. The use of fluorescent concentrators in photothermal coversion added a highlight to this session.

This set of papers serves as a timely companion and update to the SPIE Proceedings Vol. 324 of January 1982 on Optical Coatings for Energy Efficiency and Solar Applications.

Carl M. Lampert
Lawrence Berkeley Laboratory

OPTICAL MATERIALS AND PROCESS TECHNOLOGY FOR ENERGY EFFICIENCY AND SOLAR APPLICATIONS

Volume 428

Contents

OPTICAL MATERIALS AND PROCESS TECHNOLOGY FOR ENERGY EFFICIENCY AND SOLAR APPLICATIONS

Volume 428

Session 1

Heat Mirrors and Optical Switching Films

Chairmen
Gottfreid Haacke
American Cyanamid Co.
Carl M. Lampert
Lawrence Berkeley Laboratory

Optical properties of transparent and heat-reflecting Indium-Tin-Oxide films: experimental data and theoretical analysis

I. Hamberg and C.G. Granqvist

Physics Department, Chalmers University of Technology, S-412 96 Gothenburg, Sweden

Abstract

High-quality transparent and heat-reflecting Indium-Tin-Oxide films were prepared by reactive electron-beam evaporation. The complex dielectric function was evaluated from spectrophotometric measurements in the 0.25-50-μm range. The optical data are discussed from a theoretical model which encompasses the contributions from free carriers, valence electrons, and phonons. It is found that ionized impurity scattering is the main damping mechanism of the free electrons.

1. Introduction

Energy-efficient windows require coatings with high transmittance of short-wavelength radiation and high reflectance of long-wavelength radiation.[1-5] The change in the optical properties should take place at ~2 μm for a coating designed for maximum energy gain by solar radiation and minimum energy loss by outgoing thermal radiation. Alternatively, the change should occur at ~0.7 μm for a coating whose purpose is to allow visible radiation and reflect near-infrared sunlight thereby diminishing the need for air conditioning. There are several types of coatings which are capable of yielding the desired optical properties.[1,2,6] Particular interest has been focused on wide-bandgap semiconductors doped to an extent that the plasma wavelength lies in the near-infrared range.[7-9] Indium-Tin-Oxide (ITO), which is Sn-doped In_2O_3, stands out as one of the most interesting and viable alternatives.[1-6,9-18]

In earlier papers we have shown[16-18] that ITO films produced under sufficiently well-controlled conditions are capable of giving ~95 % luminous transmittance, ~10 % thermal emittance, and weak iridescence when deposited onto glass. Figure 1 shows typical spectra of transmittance (T) and reflectance (R) of a specimen consisting of a 0.36-μm-thick ITO film antireflection coated with 0.10 μm of MgF_2. The transmittance and reflectance of uncoated glass are denoted by T_g and R_g, respectively. It is found that $T \gtrsim T_g$ and $R < R_g$ over a large part of the visible range, which clearly points at the excellent quality of our transparent and heat-reflecting films. The reflectance goes up rapidly at wavelengths exceeding ~1.5 μm and is ≳ 90 % in the thermal infrared range. The results of Fig. 1 are significantly better than those of today's commercially produced coatings for energy efficient windows.

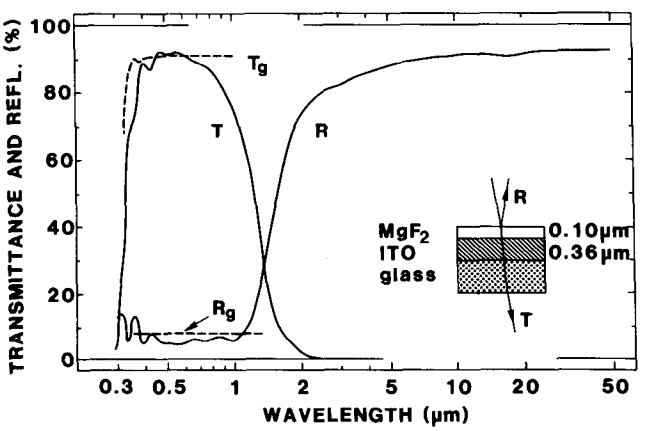

Figure 1. Transmittance and reflectance of uncoated glass (T_g and R_g; dashed curves) and of glass coated with ITO and MgF_2 as sketched in the inset (T and R; solid curves). The ITO film was produced by reactive electron-beam evaporation in 9×10^{-4} Torr of O_2 onto glass heated to 310°C; the MgF_2 film was made by resistive evaporation in good vacuum.

The main purpose of this paper is to treat the optical properties of ITO from basic principles, starting from the contributions to the dielectric function from the free carriers, the valence electrons, and the phonons. By this approach we may grasp the inherent limitations of transparent heat-mirrors of the doped semiconductor type, and we may also get an understanding of the influence from different experimental parameters on the ensuing film properties. In Sec. 2 below we give a brief presentation of the technique to prepare high quality films of ITO and In_2O_3. Section 3 gives experimental data on the complex dielectric function (ε) of doped ITO and "undoped" In_2O_3 films. In Sec. 4 we turn to the theoretical model of ε for ITO. The free electrons are treated with the approach of Gerlach and Grosse[19] as applied to ionized impurity scattering, and the susceptibility of the undoped host material is obtained from

that of pure In_2O_3. In Sec. 5 we compare experimental and theoretical data on the complex dynamical resistivity and find that ionized impurity scattering is the dominating damping mechanism of the electrons. Section 6, finally, summarizes the main results and gives some concluding remarks.

2. Film preparation and thickness measurement

Films of ITO and In_2O_3 were prepared by reactive electron-beam evaporation in a system allowing accurate process control.[16,17] The starting material was hot-pressed pellets of In_2O_3 + 9 mol. % SnO_2 and pure In_2O_3 respectively. The films were deposited onto substrates of Corning 7059 glass, calcium fluoride or silicon during a continuous inlet of oxygen. The optical quality of the coatings is known to depend critically on experimental parameters such as evaporation rate, oxygen pressure, and substrate temperature.[16,17] Optimum conditions were a rate of 0.2 to 0.3 nm/s in 5 to 8×10^{-4} Torr of O_2. The substrate temperature should exceed 150°C and preferrably lie about 300°C.

The film thickness (t) was monitored on a vibrating quartz microbalance during the evaporation. It was measured more accurately after the deposition by letting a mechanical stylus instrument scan across a region of the substrate part of which had been masked during the evaporation by a narrow strip of steel foil. The accuracy of the stylus technique is estimated to be about ±0.01 μm. A further test of t was made by optical interference in the visible spectral range and, alternatively, by combining three independent spectrophotometric recordings to determine simultaneously the complex dielectric function and t. The films employed in this study were between 0.05 and 0.5 μm thick.

3. Evaluation of the dielectric function

The spectral transmittance (T) and reflectance (R) were measured for coated and uncoated substrates on double-beam spectrophotometers with reflectance attachments and polarizers mounted in common-beam position. We used a Beckman ACTA MVII instrument in the 0.25-2.5-μm range and a Perkin-Elmer 580 B instrument at 2.5-50 μm. Both spectrophotometers were interfaced to a computer; this arrangement allowed easy storage of spectra as well as automatic computation of the complex dielectric function for a large number of data points.

Four types of data were recorded: $T_{TE}(\theta)$, $T_{TM}(\theta)$, $R_{TE}(\theta)$ and $R_{TM}(\theta)$, were θ is the angle of incidence and TE(TM) denotes transverse electric (transverse magnetic) polarization. Reference mirrors of Al, Ag, or Au were employed in the reflectance determinations. Specifically, we measured T(0), T_{TE} (45°), T_{TM} (45°), R (10°), R_{TE} (25°), and R_{TM} (25°) in the 0.25-2.5-μm interval. For the thermal infrared range we also recorded R_{TE} (60°) and R_{TM} (60°). Films on substrates of CaF_2 were used for measurements in the visible and near-infrared ranges, whereas films on Si were used in the thermal infrared.

In principle, it is straight forward to derive the complex dielectric function $\varepsilon \equiv \varepsilon_1 + i\varepsilon_2$ from two separate spectrophotometric measurements by use of Fresnel's equations[20] and the known optical properties of the substrate materials. In practice, this scheme is not always simple to apply,[21] and considerable caution is required to obtain reliable data on ε_1 and ε_2 and to avoid spurious solutions. This is so particularly when a wide spectral range is to be covered. In our evaluations, we employed carefully selected pairs of spectrophotometric input data. Literature data[22,23] on the optical properties of CaF_2 and Si were used. Films with different thicknesses had to be used to cover the 0.25-50-μm interval. Below we denote the dielectric functions of ITO and In_2O_3 by ε^{ITO} and $\varepsilon^{In_2O_3}$, respectively.

Figure 2 shows ε_1^{ITO} and ε_2^{ITO} in the visible and near-infrared spectral region for one typical film. It is seen that ε_1^{ITO} starts from ~4 in the visible and declines and becomes negative in the near-infrared. The plasma energy, corresponding to $\varepsilon_1 = 0$, occurs at 0.89 eV. ε_2^{ITO} is very low in the visible - implying that the absorptance is weak - and then increases rapidly in the infrared. The overall energy dependence of ε_1^{ITO} and ε_2^{ITO} is consistent with the expected behaviour of a free-electron plasma.

Figure 3 depicts $|\varepsilon_1^{ITO}|$ (dashed curves) and ε_2^{ITO} (solid curves) on an exponential vertical scale for the whole solar and thermal range. The data for ε_2^{ITO} pertain to three different films. We see that ε_2^{ITO} is typically below 0.05 in the visible and increases to ~500 at the far-infrared end of the spectrum. The ε_2^{ITO}-curve has different slopes at $\gtrsim$ 1 eV; this feature is of large importance for the theoretical explanation of the optical properties, as we return to shortly. The set of solid curves in Fig. 3 results from ITO films prepared under conditions which were as similar to one another as possible. Despite this fact, the data for ε^{ITO} are not quite overlapping, which points at the large sensitivity of the optical properties to even minor changes of the preparation conditions.

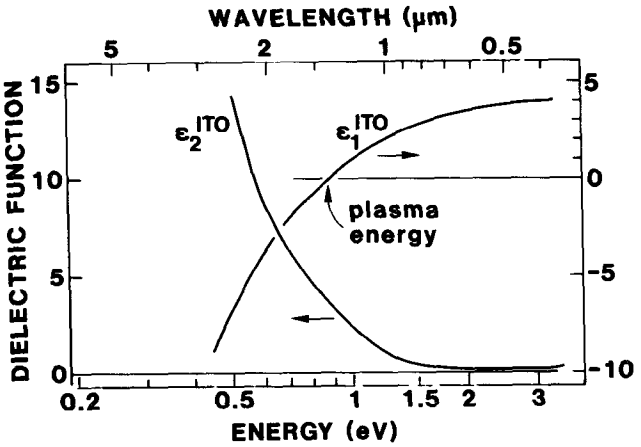

Figure 2. Real and imaginary parts of the dielectric function versus energy and wavelength for an ITO film. Note the different vertical scales for ε_1^{ITO} and ε_2^{ITO} (indicated by the arrows).

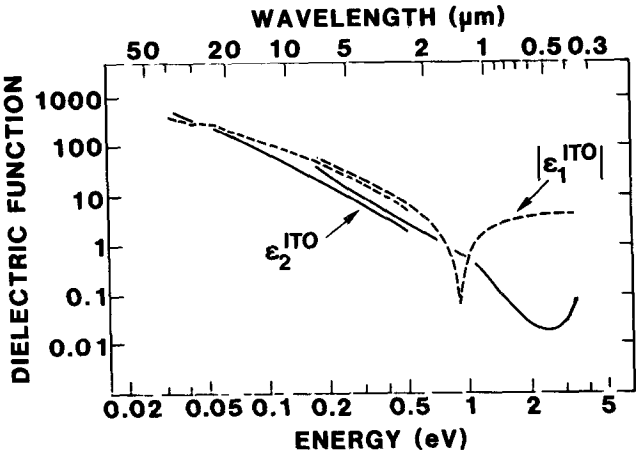

Figure 3. Real and imaginary parts of the dielectric function versus photon energy and wavelength for ITO films.

It is also of importance to analyze films of pure In_2O_3, since this material can be viewed as a host to which the effect of the Sn-dope is added in the case of ITO. It should then be noted that the dielectric function evaluated from optical measurements on evaporated In_2O_3 films cannot be immediately identified with that of the undoped host, since the specimens prepared by this technique are known[24] usually to be non-stoichiometric and display n-type conductivity as a result of doubly charged oxygen vacancies. However it is possible to subtract the effects of the autodoping by computation, as discussed in an earlier report of ours,[25] and Fig. 4 shows results representative of "undoped" In_2O_3. It is seen that $\varepsilon_1^{In_2O_3} \approx 4$ and $\varepsilon_2^{In_2O_3} \approx 0$ over the main spectral interval.[2] In the static limit, $\varepsilon_1^{In_2O_3}$ approaches 8.9. In the energy range $0.036 < h\omega < 0.056$ there appears three distinct peaks in $\varepsilon_2^{In_2O_3}$ which are associated with phonon absorption. In the high energy end there occurs a sharp increase in $\varepsilon_2^{In_2O_3}$. This feature can be related to direct-allowed transitions across a bandgap of 3.75 eV;[26] the tail towards lower energy possibly can be connected with the presence of some ionized impurities which induce a varying bandgap hence causing an absorption of the Urbach type.[27] Some evidence for such a tail was found also for ITO in Fig. 3.

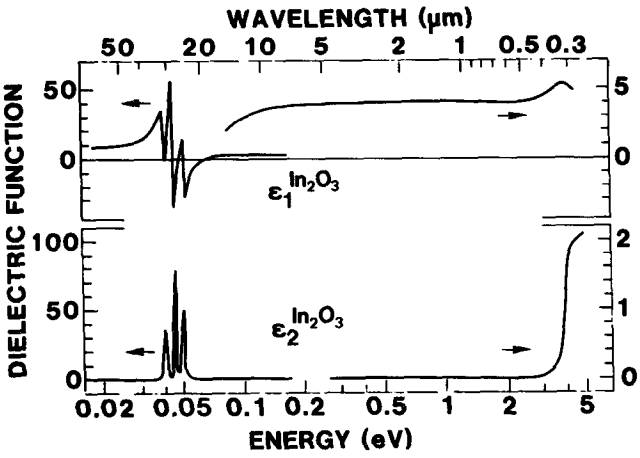

Figure 4. Real and imaginary parts of the dielectric function versus photon energy and wavelength for an In_2O_3 film. Note the different vertical scales for the high and low energy ranges.

4. Theoretical model for the optical properties

The dielectric function of a heavily doped semiconductor in most cases can be expressed as a sum of contributions from valence electrons (VE), free carriers (FC) and polar optical phonons (PH) according to[19,28]

$$\varepsilon = 1 + \chi_{VE} + \chi_{FC} + \chi_{PH}, \tag{1}$$

where χ denotes a susceptibility in SI units. We cannot distinguish between a polarization current and a current due to moving charges and hence it is meaningful to write χ in terms of a dynamic conductivity (σ) or, alternatively, a dynamic resistivity (ρ) by the relations

$$\chi(\omega) = i\frac{\sigma(\omega)}{\varepsilon_o \omega}, \tag{2}$$

$$\rho(\omega) \equiv \rho_1(\omega) + i\rho_2(\omega) = 1/\sigma(\omega), \tag{3}$$

with $\varepsilon_o = 8.84 \times 10^{-12}$ As/Vm. A description using ρ is particularly convenient because of the additivity of the different scattering processes.

The contribution from the free carriers can be accounted for within different theoretical frameworks. The simplest approach is to employ the classical Drude model, as has been done in some earlier work[16,29,30] on ITO. This theory gives

$$\rho^{Drude}(\omega) = \frac{1}{\varepsilon_o \omega_p^2 \tau} - i\frac{\omega}{\varepsilon_o \omega_p^2}, \tag{4}$$

$$\omega_p^2 = \frac{ne^2}{\varepsilon_o m^*}, \tag{5}$$

where ω_p is the plasma frequency, τ is a constant relaxation time, n is the concentration of electrons, e is the charge of the electron, and m* is its effective mass. Hence the first term in Eq. (4) is representative of the scattering and the second term stems from the inertia of the free electrons.

As we will find shortly, the Drude model is not sufficient for explaining the experimental data, but we must turn to more elaborate theories which consider explicitly the nature of the electron scattering. One theoretically sound approach is based on solutions of the Boltzmann transport equation;[31] another - somewhat more intuitive one - rests on the equivalence between energy loss and Joule heat.[32] The latter technique, which has been worked out in detail by Gerlach and Grosse,[19] is conceptually simple and leads to practically useful results; it was used in the analysis of our data on ITO. The same technique has been applied recently by Köstlin et al.[4,5,33] for treating the optical properties of ITO and doped SnO_2 within the visible and near-infrared wavelength ranges.

In the present case we regard ITO in which the Sn atoms replace some of the In atoms in the In_2O_3 lattice. These Sn atoms act in two ways: as donors giving rise to the electron plasma, and as scattering centers for the electrons. The dynamical resistivity due to ionized impurity scattering can be written as[19,34]

$$\rho(\omega) = \hat{\rho}(\omega) - i\frac{\omega}{\varepsilon_o \omega_p^2}, \tag{6}$$

$$\hat{\rho}(\omega) = i\frac{z^2 N_i}{6\pi^2 \varepsilon_o n^2 \omega}\int_0^{k_m} k^2 dk \left[\frac{1}{\varepsilon(\mathbf{k},\omega)} - \frac{1}{\varepsilon(\mathbf{k},0)}\right]. \tag{7}$$

The complex term $\hat{\rho}$ accounts for the scattering of electrons against point defects having the charge z (equal to unity in the present case) and density N_i. The point charges are taken to be screened by a dielectric function which is dependent on wavevector and frequency and which is restricted to be a linear response function. We use the longitudinal part of the Lindhard dielectric function for the degenerate electron gas.[35] The integration in Eq. (7) may then be extended to infinity as a consequence of the restrictions on the wavevectors inherent in the Lindhard expression.

The remaining part of the theoretical expression for ε is the contribution from the "undoped" In_2O_3 host lattice. To this end we identify

$$\varepsilon^{In_2O_3} = 1 + \chi_{VE} + \chi_{PH} \tag{8}$$

and use the empirical data shown in Fig. 4. The host dielectric constant is needed in the Lindhard formula; we use the value 4 in the range between the fundamental semiconductor absorption and the phonon absorption. We note that other values have been used in earlier work;[4,5,33] in our opinion there is no justification in choosing a value different from the one determined by measurements in the pertinent wavelength range.

5. Comparison of experimental and theoretical results on the complex dynamical resistivity

The purpose of this section is to compare experimental and theoretical results for the complex dielectric resistivity and to draw conclusions regarding the dominating scattering mechanism in ITO.

Figure 5 shows experimental values of ρ^{ITO} for two typical films as evaluated from the data of ε^{ITO} and $\varepsilon^{In_2O_3}$ given in Sec. 3 by use of the formulas in Sec. 4. It is seen that ρ_1^{ITO} remains constant at $\sim 3 \times 10^{-4}$ Ωcm over the main part of the shown spectral range and declines at $\hbar\omega \gtrsim 1$ eV. We find that ρ_1^{ITO} determined by optical techniques joins smoothly to the dc electrical resistivity. It is also seen that $-\rho_2^{ITO}$ goes up approximately linearly with increasing photon energy.

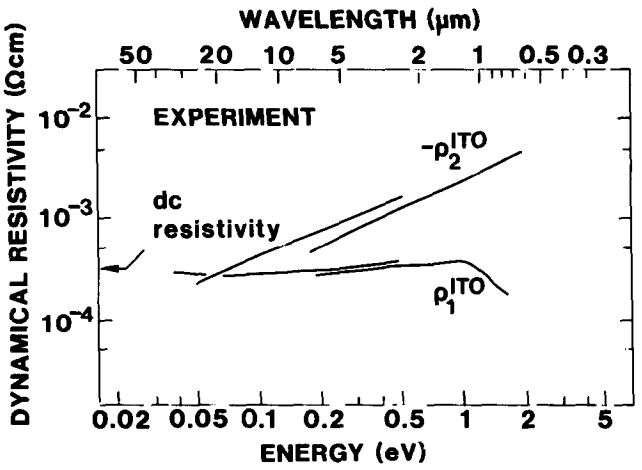

Figure 5. Experimental real and imaginary parts of the dynamical resistivity versus photon energy and wavelength for ITO films. The measured dc electrical resistivity is marked by the arrow.

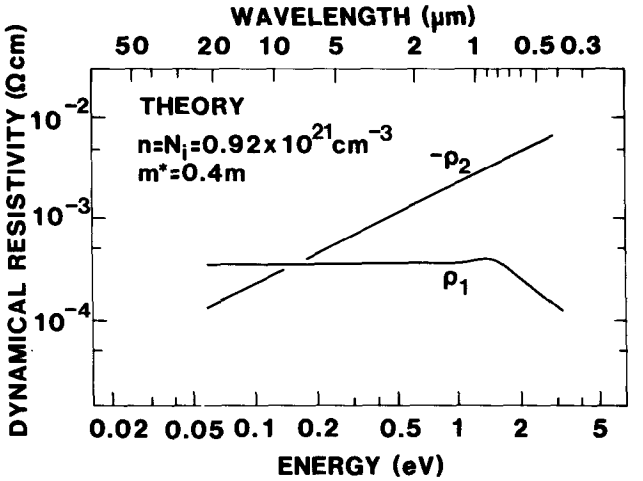

Figure 6. Theoretical real and imaginary parts of the dynamical resistivity versus photon energy and wavelength for ionized impurity scattering in an electron gas with $n = N_i = 0.92 \times 10^{21}$ cm^{-3}.

Figure 6 reports on ρ computed from the theory described in Sec. 4 and with parameters appropriate to the experimental ITO specimens. ρ_1 is shown only for $\hbar\omega > 0.06$ eV, since the effect of the phonon absorption has not yet been analyzed in detail. The calculations require specific values of n and N_i. The electron concentration was determined to 0.92×10^{21} cm^{-3} by using the experimental plasma frequency and $m^* = 0.4$ m, where m is the electron mass; the numerical factor applies to heavily doped ITO, as stated in earlier work (cf. Fig. 12 of Ref. 9). We put $n = N_i$, implying that each ionized impurity has donated one electron to the plasma. The possible role of doubly charged oxygen vacancies is neglected.

The experimental results in Fig. 5 and their theoretical counterpart in Fig. 6 are seen to be in good semi-quantitative correspondence. The linear part of ρ_1 at $\hbar\omega \lesssim 1$ eV and the $\omega^{-3/2}$-dependence at the high-energy-end both agree excellently with the experimental data, whereas the change between the two dependencies takes place at an energy which is somewhat too high for the computations. The approximate agreement between experimental ρ_1^{ITO} and theoretical ρ_1 proves that ionized impurity scattering is the dominating damping mechanism of the free electrons in our ITO films. The values of $-\rho_2$, which are proportional to ω, are also in good correspondence with the measurements. The latter data can be understood as a consequence mainly of the inertia of the free electrons, because the imaginary part of $\hat{\rho}$ was found to be negligible. Hence $-\rho_2^{ITO}$ does not give any conclusive information on the scattering.

We observe that the energy dependence of ρ_1 cannot be reconciled with the Drude model (cf. Eq. 4). Application of the Drude theory with a relaxation time determined from electrical measurements would tend to overestimate the damping in the visible spectral range. However, this effect may be balanced to some degree by an extended tail of the semiconductor bandgap.

6. Summary and concluding remarks

In this paper we have presented an experimental and theoretical analysis of the optical properties of ITO in the whole spectral range of interest for energy efficiency and solar applications. Coatings of the investigated material are highly transparent for short wavelengths and highly reflecting for long wavelengths. Furthermore, their electrical conductivity is high. These properties, together with the good substrate adherence, hardness and inertness, make ITO coatings of great interest for applications related to energy efficient windows: the coatings can provide improved thermal insulation by giving a low thermal emittance, as is wellknown, and they can also combine this property with functioning as a transparent electrode in contact with an optical switching coating of electrochromic type. Systems of the latter kind can shift reversibly from 12 to 86 % solar transmittance in short times, as has been demonstrated recently.[36]

The main conclusion of a comparison between experimental and theoretical data on the complex dynamical resistance was that ionized impurity scattering is the dominating damping mechanism. This result was obtained for heavily doped ITO, but we expect it to hold also in other materials for high-quality transparent and heat-reflecting coatings, such as doped SnO_2 and Cadmium-Tin-Oxide. Some systematic discrepancies were noted among the experimental and theoretical data. These are hardly surprising when one considers the approximations made in the theory[19] for ionized impurity scattering; for example, it regards independent point charges whereas in reality we have ions with a certain spatial extension and with a large probability of being clustered at the pertinent doping levels. It should be noted that ionized impurity scattering by no means represents the only possible damping mechanism, but scattering against neutral point defects, dislocations, grain boundaries, etc., also exists. Our analysis shows that it is feasible to produce ITO films which are sufficiently ideal that their properties are governed by the scattering of the electrons against the ions responsible for the necessary doping.

Acknowledgements

We want to thank Drs. P. Apell, E. Gerlach and H. Köstlin for informative discussions. This work was financially supported by grants from the Swedish Natural Science Research Council and the National Swedish Board for Technical Development.

References

1. C.G. Granqvist, Appl. Opt. 20, 2606 (1981).
2. C.M. Lampert, Solar Energy Mater. 6, 1 (1981).
3. G. Haacke, Proc. SPIE 324, 10 (1982).
4. G. Frank, E. Kauer, H. Köstlin, and F.J. Schmitte, Proc. SPIE 324, 58 (1982).
5. H. Köstlin, Festkörperprobleme 22, 229 (1982).
6. C.G. Granqvist, Proc. SPIE 401, to be published.
7. J.L. Vossen, Phys. Thin Films 9, 1 (1977).
8. G. Haacke, Ann. Rev. Mater. Sci. 7, 73 (1977).
9. Z.M. Jarzebski, Phys. Stat. Sol. A. 71, 13 (1982).
10. R.P. Howson and M.I. Ridge, Proc. SPIE 324, 16 (1982).
11. W.-D. Dachselt, W.-D. Münz, and M. Scherer, Proc. SPIE 324, 37 (1982).
12. J. Ebert, Proc. SPIE 325, 29 (1982).
13. W.C. Kittler, Jr. and I.T. Ritchie, Proc. SPIE 325, 61 (1982).
14. W.-D. Münz and S.R. Reineck, Proc. SPIE 325, 65 (1982).
15. J.C. Manifacier, Thin Solid Films 90, 297 (1982).
16. I. Hamberg, A. Hjortsberg, and C.G. Granqvist, Appl. Phys. Lett. 40, 362 (1982).
17. I. Hamberg, A. Hjortsberg, and C.G. Granqvist, Proc. SPIE 324, 31 (1982).
18. I. Hamberg and C.G. Granqvist, Appl. Opt. 22, 609 (1983).
19. E. Gerlach and P. Grosse, Festkörperprobleme 17, 157 (1977).
20. M. Born and E. Wolf, Principles of Optics, 5th edition (Pergamon, New York, 1975).
21. A. Hjortsberg, Appl. Opt. 20, 1254 (1981).
22. Data supplied by the Harshaw Chemical Company.
23. C.D. Salzberg and J.J. Villa, J. Opt. Soc. Am. 47, 244 (1957).
24. G. Frank and H. Köstlin, Appl. Phys. A27, 197 (1982).
25. I. Hamberg and C.G. Granqvist, Thin Solid Films, to be published.
26. R.L. Weiher and R.P. Ley, J. Appl. Phys. 37, 299 (1966).
27. N.F. Mott and E.A. Davis, Electronic Processes in Non-Crystalline Materials, 2nd edition (Clarendon, Oxford, 1979), p. 273.
28. See, for example, G.D. Mahan, Many-Particle Physics (Plenum, New York, 1981), p. 543.

29. J.C.C. Fan and F.J. Bachner, J. Electrochem. Soc. 122, 1719 (1975); Appl. Opt. 15, 1012 (1976).
30. Y. Ohhata and S. Yoshida, Oyo Butsuri 46, 43 (1977); S. Yoshida, Appl. Opt. 17, 145 (1978).
31. D. Chattopadhyay and H.J. Queisser, Rev. Mod. Phys. 53, 745 (1981).
32. M.G. Calkin and P.J. Nicholson, Rev. Mod. Phys. 39, 361 (1967).
33. P. Grosse, F.J. Schmitte, G. Frank and H. Köstlin, Thin Solid Films 90, 309 (1982).
34. E. Gerlach, Phys. Stat. Sol. B 61, K97 (1974).
35. J. Lindhard, Kgl. Danske Videnskab. Selskab, Mat.-Fys. Medd. 28, No. 8 (1954).
36. J.S.E.M. Svensson and C.G. Granqvist, to be published.

Industrial realization of low-emittance oxide/metal/oxide films on glass

K. Hartig, W.D. Münz, M. Scherer*, V. Wittwer, Stahl**

*Leybold-Heraeus GmbH, Wilhelm-Rohn-Str. 25,D-645 Hanau,**Fraunhofer Institut,D-7800 Freiburg

Abstract

Energy consumption can be reduced from room heating using coated architectural glass panes.[1] With a system oxide/metal/oxide high transmittance in the visible as well as high reflectance in the thermal infrared can be achieved[2-7]. This heat mirrors can be deposited economically by diode- and high rate sputtering. Of most interest are heat mirrors based on Cu, Ag and Au coatings. In the visible Au and Cu show a remarkable amount of absorptance which leads to a clear decrease in visible light transmittance. Best results are obtained with Ag based coatings. Ag is still high reflective even at the near U-V region. This part of reflected energy can be converted to transmittance by a properly designed optical interference stack of the type oxide/metal/oxide. For a single pane an average value of visible light transmittance between 380 nm and 780 nm of 81 % is possible without loss of infrared reflectance at 8 µm below 90 % which corresponds to a low-emittance of 0.1. For this high quality a smooth growth of the Ag layer is necessary. Experiments have shown that a bombardement of the Ag layer with high energetic ions must be avoided as far as possible.

Introduction

The main purpose of low-e coatings is to save energy. On the other hand the main purpose of a window is to have a visible light transmittance as high as possible. Therefore it is no solution of the problem to have an excellent K-value and nearly no visible transmittance left. The K-value at least determines the heat-losses through a window unit. The lower the K-value the lower the losses. The quality of a low-e coating is therefore given by a combination of both, transmittance in the visible and reflectance in the far infrared.

In this paper differences between Au- and Cu- and on the other hand Ag based coatings will be discussed. The realization and the advantages of the Ag based coatings with high quality are shown.

Comparison between different low-e coatings in the market

Fig. 1 shows K-values of different low-e coatings in the market (or at samples available). The calculations are based on measured infrared reflectivities assuming the same conditions for the double glazing like airspace, gas-filling, indoor/outdoor conditions.

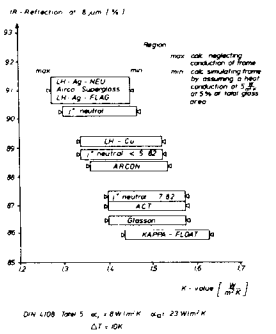

Figure 1. K-value calculations of double glazed windows.(Ar filling,12 mm distance)

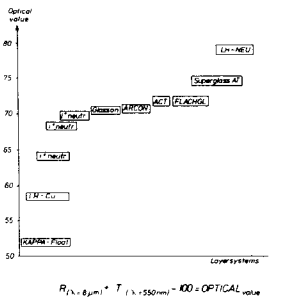

Figure 2. Combined optical and infrared performance of low-e coatings

The lower results neglect the heat conduction by the frame for a 1 by 1 m² window. K-values between 1,3 and 1,5 W/m²K are common and strongly correlated to the infrared reflectance. Two systems are based on Cu (LH-Cu, Kappa Float), while all the others are based on silver.

To compare the different low-e coatings in Fig. 2 a so called "optical value" is defined, which combines the transmittance in the visible and the infrared reflectance:

$$\text{Optical value} = R_{(\lambda = 8\ \mu m)} + T_{(\lambda = 550\ nm)} - 100$$

The optical values of the silver systems indicate that there must be big differences in quality. Systems with the same infrared reflectance differ in the optical values by nearly 10 %! Between Cu- and Ag-based coatings there is a basic difference. While Cu-coatings in the maximum reach 60 %, Ag coatings reach 80 %!

The reason for this shows Fig.3. The reflectance of Au, Cu and Ag are compared for optical dense films as a function of wavelength [8]. In the far infrared the reflectance is equal and reaches about 98 %. In the visible Au and Cu show a remarkable amount of absorptance while Ag is still high reflective even at the near UV-region. This part of reflected energy might be converted to transmission by a properly designed optical interference stack of the type oxide/metal/oxide/glass.

This is the reason for concentration on Ag-systems in this paper because we want a window should stay as transparent as possible.

One point has to be noticed. For both the Cu- and the Ag-system the effective solar energy transfer into the building is nearly the same. In the case of Ag most of the energy is directly transmitted into the building while in the case of Cu one part of the energy is absorbed by the Cu, converted to the thermal energy and then emitted to a percentage of 90 % into the building.

Silver based low-e coatings of high quality

In Fig. 4 the transmittance and reflectance for one 100 Å thick Ag layer are compared to an optimized 3-layer system oxide/Ag/oxide. Maximum transmission of 87 % in the visible are possible without loss of infrared reflectance at 8 µm below 90 %. The region of high transparency is not too small giving a good total solar energy transmittance and allows the production of a neutral reflection colour of the coating. If a special colour in reflection is wanted this may be achieved by variation in the thickness of the oxide top coat.

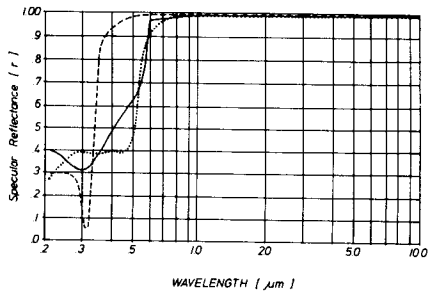

Figure 3. Specular reflectance curves for a number of metal films: Au -, Ag--, Cu...

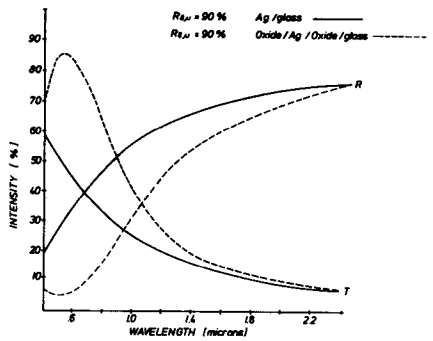

Figure 4. Effect of antireflective coating on Ag

To get this high quality coating two points are especially important. The first one is to produce a fully oxidized dielectric layer. If it is not stochiometric extra absorption will appear.

Normally the reactive sputtering of non absorbing oxides is no problem. But in order to get a high deposition rate the oxygen flow for the reactive process has to be minimized[9]. At this point the danger of non stochiometric, absorbing oxide is high. The results for this behaviour are shown in Fig. 5 for two ITO/Ag/ITO layer systems.

In one case the absorption leads to a remarkable change of colour and transmittance while the infrared reflectance stays unchanged.

The second point which may also influence the quality of the coating is the Ag itself, even if the nominal thickness of the Ag stays constant. If the Ag-layer breaks up into unconnected islands the infrared reflectance drops and scattering of light at the Ag-particals causes loss of transmittance. Such a behaviour shows Fig. 6a. A SEM is taken from a magnetron sputtered Ag coating, 100 Å nominal thickness on ITO. The surface roughness in connection with the measured loss of electrical conductivity has to be interpreted as formation of islands of Ag.

This is a well known behaviour of especially Ag on dielectric substrates under special conditions.

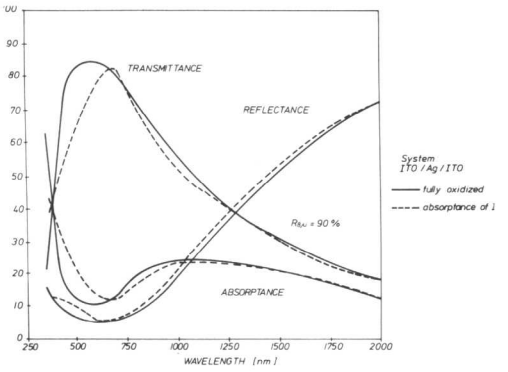

Figure 5. Transmittance, reflectance and absorptance of ITO/Ag/ITO on glass - fully oxidized ITO,---absorptance of ITO

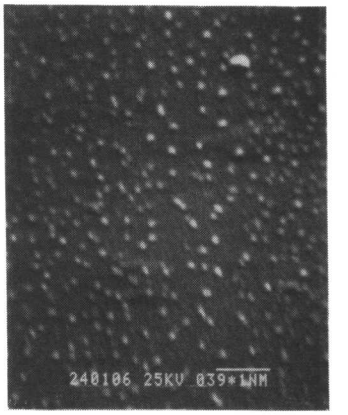

Figure 6 . Structure of silver layers a. Formation of clusters: High-energy level

The nucleation theory as well as experiments show that the clustering of Ag is extremely dependant on the substrate temperature. The higher the temperature the lesser and bigger clusters will be built.

Fig. 7 shows the size of clusters for a nominal 100 Å thick Ag layer evaporated on to a substrate at a temperature of 350 °C[10]. In this case cluster sizes of about 6000 Å will appear while the density is very low.

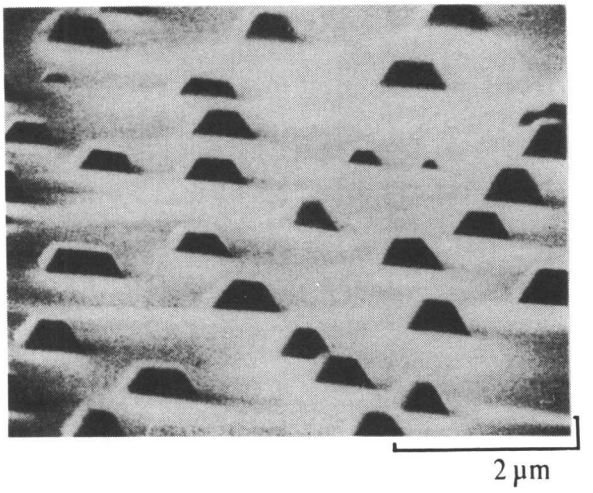

Figure 7. Size and density of Ag clusters for a nominal 100 Å thick Ag layer deposited on Ag <100> at a surface temperature of 350 °C.

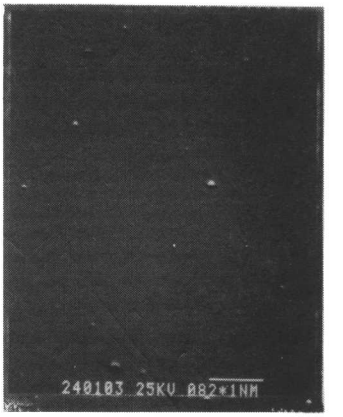

Figure 6 . Structure of silver layers b. Smooth growth : Low energy level

In Fig. 8 the variation of cluster sizes in the temperature range between 30 °C and 600°C is given [10] . This is valid for evaporation but shows that the size grows fast with the temperature. If extra energy is added to the surface by impact of energetic ions, as it happens during sputter processes the given scale of substrate temperatures might be shifted to lower values. This indicates that during the sputtering of the Ag layer or the oxide top layer a bombardement of high energetic ions must be avoided as far as possible (Fig. 6b).

For the realization of low-e coatings magnetron sources as well as diode sources are possible and under very good use. Classical diode sputtering is often thought to be a source of high energetic particals.

Experiences with production coaters using this principle under optimized conditions show that there is almost no difference in quality of Ag layer systems compared to results of magnetron sputtering.